

The Phoenix Deep Survey: X-ray properties of faint radio sources

A. Georgakakis^{1*}, A. M. Hopkins^{2†}, M. Sullivan³, J. Afonso⁴, I. Georgantopoulos¹
B. Mobasher⁵, L. E. Cram⁶

¹ *Institute of Astronomy & Astrophysics, National Observatory of Athens, I. Metaxa & B. Pavlou, Penteli, 15236, Athens, Greece*

² *Department of Physics and Astronomy, University of Pittsburgh, 3941 O'Hara Street, Pittsburgh, PA 15260, USA*

³ *Physics Department, University of Durham, Science Labs, South Road, Durham, DH1 3LE*

⁴ *Centro de Astronomia e Astrofísica da Universidade de Lisboa, Observatório Astronómico de Lisboa, Tapada da Ajuda, 1349-018 Lisboa, Portugal*

⁵ *Space Telescope Science Institute, 3700 San Martin Drive, Baltimore, MD 21218, USA*

⁶ *Australian Research Council, GPO Box 9880, Canberra ACT 2601, Australia*

2 February 2008

ABSTRACT

In this paper we use a 50 ks XMM-*Newton* pointing overlapping with the Phoenix Deep Survey, a homogeneous radio survey reaching μJy sensitivities, to explore the X-ray properties and the evolution of star-forming galaxies. Multiwavelength UV, optical and near-infrared photometric data are available for this field and are used to estimate photometric redshifts and spectral types for all radio sources brighter than $R = 21.5$ mag (total of 82). Faint radio galaxies with $R < 21.5$ mag and spiral galaxy SEDs (total of 34) are then segregated into two redshift bins with a median of $z = 0.240$ (total of 19) and 0.455 (total of 15) respectively. Stacking analysis for both the 0.5–2 keV and 2–8 keV bands is performed on the two subsamples. A high confidence level signal ($> 3.5\sigma$) is detected in the 0.5–2 keV band corresponding to a mean flux of $\approx 3 \times 10^{-16} \text{ erg s}^{-1} \text{ cm}^{-2}$ for both subsamples. This flux translates to mean luminosities of $\approx 5 \times 10^{40}$ and $\approx 1.5 \times 10^{41} \text{ erg s}^{-1}$ for the $z = 0.240$ and 0.455 subsamples respectively. Only a marginally significant signal (2.6σ) is detected in the 2–8 keV band for the $z = 0.455$ subsample. This may indicate hardening of the mean X-ray properties of sub-mJy sources at higher redshifts and/or higher luminosities. Alternatively, this may be due to contamination of the $z = 0.455$ subsample by a small number of obscured AGNs. On the basis of the observed optical and X-ray properties of the faint radio sample we argue that the stacked signal above is dominated by star-formation with the AGN contamination being minimal. The mean X-ray-to-optical flux ratio and the mean X-ray luminosity of the two subsamples are found to be higher than optically selected spirals and similar to starbursts. We also find that the mean X-ray and radio luminosities of the faint radio sources studied here are consistent with the $L_X - L_{1.4}$ correlation of local star-forming galaxies. Moreover, the X-ray emissivity of sub-mJy sources to $z \approx 0.3$ is estimated and is found to be elevated compared to local H II galaxies. The observed increase is consistent with X-ray luminosity evolution of the form $\approx (1+z)^3$. Assuming that our sample is indeed dominated by star-forming galaxies this is direct evidence for evolution of such systems at X-ray wavelengths. Using an empirical X-ray luminosity to star-formation rate (SFR) conversion factor we estimate a global SFR density at $z \approx 0.3$ of $0.029 \pm 0.007 M_\odot \text{ yr}^{-1} \text{ Mpc}^{-3}$. This is found to be in fair agreement with previous results based on galaxy samples selected at different wavelengths.

Key words: Surveys – Galaxies: normal – X-rays:galaxies – X-ray:general

* email: age@astro.noa.gr

† Hubble Fellow

1 INTRODUCTION

Deep X-ray surveys with the *Chandra* observatory (Brandt et al. 2001a; Mushotzky et al. 2000) have demonstrated beyond any doubt the appearance of ‘normal’ (i.e. non-AGN dominated) star-forming galaxies at faint flux limits, $f(0.5 - 2 \text{ keV}) \approx 10^{-16} \text{ erg s}^{-1} \text{ cm}^{-2}$ (Brandt et al. 2001b; Hornschemeier et al. 2002a; Alexander et al. 2002; Bauer et al. 2002). These systems are detected in increasing numbers with decreasing X-ray flux and are likely to outnumber AGNs below $f(0.5 - 2 \text{ keV}) \approx 10^{-17} \text{ erg s}^{-1} \text{ cm}^{-2}$ (Hornschemeier et al. 2002b; Ranalli, Comastri & Setti 2003). The steeply increasing X-ray source counts of star-forming galaxies also suggest evolution. Our knowledge on this key issue, however, remains sparse. Theoretical models predict moderate to strong X-ray evolution for these systems at $z < 1$ (Ghosh & White 2001) but a tight observational constraint remains to be obtained. Brandt et al. (2001b) studied the mean X-ray properties of bright spirals at $z \approx 0.5$ using the 500 ks *Chandra* exposure of the HDF-North. They find that the mean X-ray luminosity of their sample is elevated compared to local spirals suggesting evolution consistent with the Ghosh & White (2001) models. Differences between the L_B distribution of their sample and that of local spirals, however, may also be responsible for the observed increase. Hornschemeier et al. (2002a) used stacking analysis to investigate the mean properties of $z \approx 1$ spirals in the *Chandra* Deep Field North. They found evidence for an increase in the mean L_X/L_B ratio compared to local star-forming systems. Statistical uncertainties, however, did not allow firm conclusions to be drawn.

Clearly these studies, although of key significance for understanding the X-ray properties of star-forming galaxies at moderate to high redshifts, cannot strongly constrain their evolution. To address this issue a number of observational challenges need to be resolved. Firstly, distant starbursts are X-ray faint and therefore their detection even with the *Chandra* and the XMM-*Newton* observatories is difficult. More importantly compiling starburst galaxy samples with well defined selection criteria over a wide redshift range is not trivial.

The aim of this paper is to address these issues to provide a direct observational constraint on the X-ray evolution of star-forming galaxies. We combine data from an ultra-deep and homogeneous radio (1.4 GHz) survey (the Phoenix Deep Survey; Hopkins et al. 2003) to the limit $S_{1.4} = 80 \mu\text{Jy}$ (5σ) with a single deep (50 ks) XMM-*Newton* pointing covering an area of 30 arcmin diameter. Compared to previous studies this dataset, the Phoenix/XMM survey, has the advantage of deep wide area μJy radio observations. Such observations have been shown to be efficient in identifying actively star-forming galaxies to $z \approx 1$ with small contamination by AGNs (10–20 per cent; Georgakakis et al. 1999; Barger 2002; Bauer et al. 2002; Chapman et al. 2003). Also, the insensitivity of radio wavelengths to dust obscuration suggests that deep radio surveys are unique for compiling starburst samples to $z \approx 1$ with uniform selection criteria free from dust induced biases. A minor drawback of radio selection is that it may underestimate the SF activity in low luminosity galaxies ($\approx 0.01 L_*$; Condon et al. 1992; Bell 2003; Chapman et al. 2003). These systems are believed to substantially contribute to the star-formation rate density

in the local universe (e.g. Wilson et al. 2002). Keeping this caveat in mind, the Phoenix/XMM survey still offers an excellent opportunity to explore the X-ray evolution of star-forming galaxies.

Section 2 presents the multiwavelength data available for the Phoenix Deep Survey, section 3 describes the X-ray data while section 4 details the sample used in the present study. The stacking technique is outlined in section 5, and the results are presented in section 6. Section 7 argues against AGN contamination of the present radio selected sample while our results are discussed in section 8. Finally, section 9 summarises our conclusions. For comparison with previous studies throughout this paper we adopt $H_0 = 65 \text{ km s}^{-1} \text{ Mpc}^{-1}$ and $q_0 = 0.5$ but we also give results for the $\Omega_M = 0.3$, $\Omega_\Lambda = 0.7$ and $H_0 = 65 \text{ km s}^{-1} \text{ Mpc}^{-1}$ cosmology.

2 THE PHOENIX DEEP SURVEY

The Phoenix Deep Survey (PDS) is an on-going program aiming to study the nature and the evolution of sub-mJy and μJy radio galaxies. The radio observations were carried out at the Australia Telescope Compact Array (ATCA) at 1.4 GHz during several campaigns between 1994 and 2001 in the 6A, 6B and 6C array configurations. The data cover a 4.56 square degree area centered at RA(J2000)= $01^{\text{h}}11^{\text{m}}13^{\text{s}}$ Dec.(J2000)= $-45^\circ 45' 00''$. A detailed description of the radio observations, data reduction and source detection are discussed by Hopkins et al. (1998, 1999, 2003). The observational strategy adopted resulted in a radio map that is highly homogeneous within the central ≈ 1 deg radius. Nevertheless, the 1σ rms noise increases from $12 \mu\text{Jy}$ at the most sensitive region to about $90 \mu\text{Jy}$ close to the field edge. The final catalogue consists of a total of 2058 radio sources to a limit of $60 \mu\text{Jy}$ (5σ ; Hopkins et al. 2003).

Follow-up optical photometric observations of the entire PDS in the *V* and *R*-bands were obtained at the Anglo-Australian Telescope (AAT) during two observing runs in 1994 and 1995 September. A detailed description of these observations including data reduction, photometric calibration, source extraction and optical identification are presented by Georgakakis et al. (1999). In brief, this dataset is complete to $R = 22.0$ mag and allows optical identification of about 50 per cent of the radio sample. An on-going spectroscopic program aiming to obtain spectral information for the optically identified sources is underway using the 2dF facility at the AAT. At present redshifts and spectral classifications are available for over 300 sources brighter than $R = 21.5$ mag. This optical magnitude limit is the only selection applied to the radio sample for follow-up spectroscopy. Part of this large dataset is presented by Georgakakis et al. (1999). Galaxies are grouped on the basis of spectral features and diagnostic emission-line ratios into (i) systems exhibiting absorption-line features only, (ii) star-forming galaxies, (iii) narrow emission line Seyfert 2s, (iv) broad line Seyfert 1s and (v) ‘unclassified’ objects. The latter have at least one narrow emission line identified in their optical spectra (allowing redshift determination) but the poor S/N ratio, or the small number of emission lines within the observable window, or the presence of instrumental features contami-

nating emission lines prevented a reliable spectral classification (Georgakakis et al. 1999).

A new set of high quality deep multiwavelength *UBVRI* photometric data has recently been obtained for a subregion of the PDS partly overlapping with the Phoenix/XMM field using the Wide Field Imager at the AAT (*BVRI*-bands) and the ESO 2.2 m (*U*-band) telescopes complete to $I \approx 24$ and $U \approx 22.5$ mag respectively. Near-infrared (NIR) photometric observations (J and K -bands) complete to $K \approx 18$ mag have also been obtained for the 30 arcmin diameter area of the Phoenix/XMM survey using OSIRIS at the CTIO 1.5 m telescope. The UV, optical and NIR data will be presented in a series of forthcoming papers.

3 THE X-RAY DATA

A subregion of the PDS centered at RA(J2000)=01^h12^m52^s; Dec.(J2000)=−45°33′10.0″ was surveyed by the XMM-Newton on 2002 May 5. The observation consists of a single pointing with an exposure time of ≈ 50 ks. The EPIC (European Photon Imaging Camera; Strüder et al. 2001; Turner et al. 2001) cameras were operated in full frame mode with the medium filter applied.

The XMM-Newton data have been analysed using the Science Analysis Software (SAS 5.3). Event files for the PN and the two MOS detectors have been produced using the EPCHAIN and EMCHAIN tasks of SAS respectively. The event files were screened for high particle background periods by rejecting times with 0.5–10 keV count rates higher than 20 and 6 cts/100s for the PN and the two MOS cameras respectively. The adopted count rates are a trade off between maximum effective exposure time and low particle background contamination. Higher thresholds do not significantly increase the exposure time while lower thresholds severely reduce the effective exposure time. The PN and MOS good time intervals are 39444 and 41273 s respectively. The difference between the PN and the MOS exposure times is due to varying start and end times of the detectors. Only events corresponding to patterns 0–4 for the PN and 0–12 for two MOS cameras have been kept. To increase the signal-to-noise ratio and to reach fainter fluxes the PN and the MOS event files have been combined into a single event list using the MERGE task of SAS.

Images in celestial coordinates with pixel size of 4.35 arcsec have been extracted in the spectral bands 0.5–8 keV (total), 0.5–2 keV (soft) and 2–8 keV (hard) for the merged event file. Events with energies below 0.5 or above 8 keV are not used here because of the reduced XMM-Newton effective area at these energies. Also, below 0.5 keV the background is elevated due to the Galactic X-ray emission component (Lumb et al. 2002). Therefore, photons with energies < 0.5 and > 8 keV primarily increase the background and do not improve the signal-to-noise ratio of the final image. Exposure maps accounting for vignetting, CCD gaps and bad pixels have been constructed for each spectral band.

Source detection was independently performed in the total (0.5–8 keV), soft (0.5–2 keV) and hard (2–8 keV) band images using the EWAVELET task of SAS with a significance threshold of 4σ . A byproduct of the source extraction algorithm is the construction of background maps

for each spectral band. We detect 137, 128 and 88 X-ray sources in the 0.5–8, 0.5–2 and 2–8 keV spectral bands respectively. The 4σ limiting fluxes in these spectral bands are $f(0.5–8 \text{ keV}) \approx 10^{-15}$, $f(0.5–2 \text{ keV}) \approx 9 \times 10^{-16}$ and $f(2–8 \text{ keV}) \approx 2 \times 10^{-15} \text{ erg s}^{-1} \text{ cm}^{-2}$. A small number of X-ray faint sources are only detected in either the soft (total of 11) or the hard (total of 9) bands and are missed from the total band due to the elevated background. A detailed analysis of the nature of the X-ray sources detected in the Phoenix/XMM survey will be presented in a forthcoming paper (Georgakakis et al. in preparation). To convert counts to flux the Energy Conversion Factors (ECF) of individual detectors are calculated assuming a power law spectrum with $\Gamma = 2.0$ (e.g. Bauer et al. 2002) and Galactic absorption $N_H = 2 \times 10^{20} \text{ cm}^{-2}$ appropriate for the PDS. The mean ECF for the mosaic of all three detectors is estimated by weighting the ECFs of individual detectors by the respective exposure time. For the encircled energy correction, accounting for the energy fraction outside the aperture within which source counts are accumulated, we adopt the calibration performed by Ghizzardi (2001a, 2001b). These studies use both PN and MOS observations of point sources to formulate the XMM-Newton PSF for different energies and off-axis angles. In particular, a King profile is fit to the data with parameters that are a function of both energy and off-axis angle. The encircled energy correction for the merged PN+MOS image is estimated by weighting the corrections of individual detectors by the respective exposure time. In any rate the difference between the PN and MOS encircled energy corrections found by Ghizzardi (2001a, 2001b) is negligible.

4 THE RADIO SAMPLE

A total of 204 radio sources lie within the 30 arcmin diameter region covered by the Phoenix/XMM survey. This field lies within the most homogeneously covered region of the PDS but is offset from the most sensitive area of the radio map by about 0.30 deg. Therefore, the completeness limit of the radio observations in that 30 arcmin diameter region is $\approx 80 \mu\text{Jy}$ (5σ). A total of 82 out of the 204 radio sources have optical counterparts brighter than $R = 21.5$ mag. Of the 82 sources with $R < 21.5$ mag a subsample of 31 have spectroscopic data and secure redshifts. The spectroscopic sample comprises 7 absorption-line systems likely to be E/S0, 10 star-forming galaxies, 1 broad-line AGN, 1 Seyfert-2 and 12 “unclassified” narrow emission line sources. As discussed in section 2, the latter group of galaxies have poorly constrained optical spectral properties and their nature (AGN, star-formation) remains uncertain. In the next section we discuss evidence suggesting that although some of these sources are expected to be AGNs, many (especially at $z < 0.4$) are likely to be starbursts.

For the remaining radio sources with $R < 21.5$ mag and no spectroscopic information (total of 61) we exploit the existing broad-band data (*UBVRIJK*) to estimate photometric redshifts using the HYPER-Z code (Bolzonella, Miralles & Pelló 2000). The HYPER-Z program determines the photometric redshift of a given object by fitting a set of template Spectral Energy Distributions (SEDs) to the observed photometric data through a standard χ^2 minimisation tech-

nique. The template rest-frame SEDs used here are the observed mean spectra of four different galaxy types (E/S0, Sbc, Scd, Im) from Coleman, Wu & Weedman (1980) extended in the UV and IR regions using the spectral synthesis models of Bruzual & Charlot (1993) with parameters selected to match the observed spectra.

Figure 1 compares the photometric and spectroscopic redshift estimates of the 31 objects with available spectroscopic observations. The agreement is good with $(z_{\text{phot}} - z_{\text{spec}})/z_{\text{spec}} \approx 0.09$. Moreover, Figure 1 shows there is a fair agreement between the observed spectral classification (emission, absorption line) and the galaxy type of the best fit SED (ellipticals, spirals, irregulars). Figure 2, plots the photometric and spectroscopic redshift distributions of the $R < 21.5$ radio sample. It is clear that the agreement between the two distributions is good suggesting that the photometric redshift estimates are reliable.

We find that the majority of the sub-mJy sources are best fit by late-type SEDs in agreement with previous studies suggesting that the faint radio population is dominated by star-forming spirals. We find 65 systems with spiral/irregular type SEDs and 17 radio sources with elliptical best fit SEDs with redshifts in the range 0.05–2.0 and 0.05–0.6 respectively. The present radio selected sample also includes one broad-line AGN at $z \approx 1.9$ that is assigned an irregular galaxy SED and a photometric redshift of ≈ 1.7 . Despite the agreement, the galaxy SEDs used here are not suitable to either estimate QSO photometric redshifts or to identify such sources within the sample. In the absence of optical spectroscopy distant QSOs can be identified by their unresolved optical light profile. A total of 7 radio sources have optical counterparts that are unresolved in the R -band images and are excluded from the analysis as QSO candidates. In summary out of 82 radio sources with $R < 21.5$ 65 have spiral/irregular SEDs and 17 have E/S0 SEDs. Of the 65 sources with spiral/irregular SEDs a total of 3 have unresolved optical light profiles and 1 is a spectroscopically confirmed QSO. Of the 17 sources with E/S0 SEDs a total of 4 have unresolved optical light profiles.

5 STACKING PROCEDURE

Stacking methods have been extensively used in X-ray astronomy to study the mean properties (e.g. flux, luminosity, hardness ratios) of well defined samples of sources that are otherwise too faint at X-ray wavelengths to be individually detected (e.g. Nandra et al. 2002).

In practice, the X-ray counts (source-plus-background) at the position of each galaxy in the sample are added excluding X-ray detected galaxies. The expected background contribution is estimated by summing the counts from regions around each source. Assuming Poisson statistics for the counts a significance level is estimated for the summed signal.

To determine the size of the region within which the source-plus-background counts are extracted we adopt the empirical method described by Nandra et al. (2002). Tests are performed in which the radius of the circular aperture within which the source-plus-background counts are summed varies (from one trial to the next) between 6–18 arcsec. We find that a radius of 10 arcsec maximises the

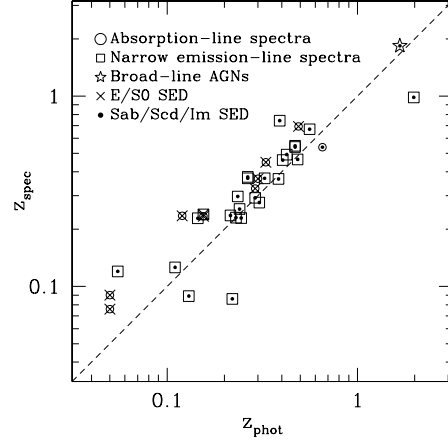


Figure 1. Photometric against spectroscopic redshift estimates for the 31 sub-mJy radio sources with available spectroscopic observations. Open circles are radio galaxies with absorption line spectra, open squares correspond to systems with narrow-emission line spectra and stars are broad line AGNs. A cross on top of a symbol indicates an E/S0 best fit SED to the photometric data, while small dots are for Sab, Sbc or Im SEDs. There is good agreement between photometric and spectroscopic redshifts and between the spectral classification (absorption or emission line spectra) and the galaxy type of the best fit SED.

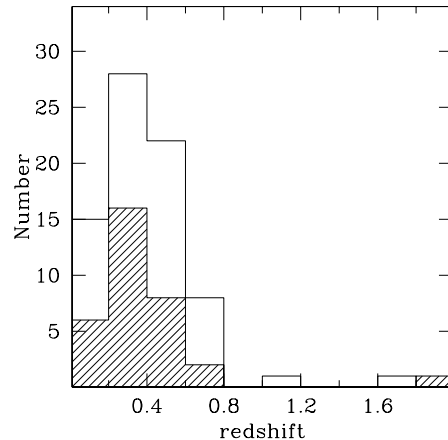


Figure 2. Redshift distributions of the sub-mJy radio sources with spectroscopic (hatched histogram) and photometric redshifts.

significance of the stacked signal and hence this optimal extraction radius is adopted for the analysis that follows. This extraction radius is about 2.5 times the on-axis HWHM of the XMM-Newton PSF (Hasinger et al. 2001). To assess the significance of the stacked signal we estimate the background from (i) the smooth background maps produced by the EWAVELET task of SAS using 20 arcsec annuli centered on the sample galaxies and (ii) the science images by taking the average of 60 10 arcsec apertures randomly positioned within annular regions centered on the positions of the sample galaxies with inner and outer radii of 20 and 100 arcsec respectively. In the latter method regions close to

X-ray sources (< 40 arcsec) are excluded to avoid contamination from X-ray detections in the background estimation. We find that the significance of the stacked signal does not depend on the background estimation method. For simplicity we use the background maps to estimate the mean background. We note that the size of the background aperture does not modify our results.

To further assess the confidence level of the stacked signal we perform extensive simulations: mock catalogs are constructed by randomising the positions of the radio sample avoiding areas close to X-ray sources (< 40 arcsec). Each of the mock catalogs has the same number of sources as the real radio catalog. We then apply the stacking analysis to the mock catalogs and estimate the significance of the stacked signal in the same way as in the real catalog. This is then repeated 10 000 times to get the distribution of the detection significances for the mock catalogs. This provides an estimate of the probability of getting a statistically significant stacked signal by chance. The detection confidence levels estimated from the simulations are in excellent agreement with those based on Poisson statistics

In practice we have excluded from the stacking analysis galaxies that are identified with X-ray sources detected by the EWAVELET task to the 4σ significance level. Such a low detection threshold is essential to study the mean properties of X-ray weak sources, the signal of which would otherwise be diluted by brighter ones. We find 9 radio sources with X-ray counterparts within 8 arcsec off the radio position: 4 of them have narrow emission-line spectra, while the rest have no spectroscopic information but their broad band colours suggest spiral galaxy SEDs. Most of these X-ray detected radio sources have hard X-ray spectra and X-ray luminosities of $\approx 10^{43}$ erg s $^{-1}$ suggesting AGN activity rather than star-formation. A detailed study of these radio sources will be presented in a forthcoming paper.

Moreover, counts associated with the wings of the PSF of bright X-ray sources might erroneously increase the stacking signal significance. Therefore, to avoid contamination of the stacking signal from nearby X-ray sources we have excluded from the analysis a total of 12 radio galaxies that lie close (i.e. 8–40 arcsec) to X-ray detections. A total of 21 radio sources, either lying close to (12 objects; 8–40 arcsec) or being associated with (9 objects; < 8 arcsec) X-ray detections, have thus been excluded.

The aim of the present paper is to explore the mean properties of star-forming sub-mJy radio galaxies. Our sample is restricted to sub-mJy sources with $S_{1.4} > 80 \mu\text{Jy}$ (the flux density limit of the radio catalogue) and spiral galaxy SEDs that are not associated with or do not lie close to X-ray sources. Further, in the analysis that follows we use only radio sources with redshift $z < 0.8$, since at higher redshifts the present sample with $R < 21.5$ becomes highly incomplete. We also exclude distant AGNs as explained above. The final sample used in the stacking analysis comprises 34 radio galaxies that fulfill the above criteria.

6 RESULTS

The sub-mJy radio sources used in the stacking analysis are split into two independent redshift bins $z = 0.0 - 0.3$ and $z = 0.3 - 0.8$ with median redshifts of 0.240 and 0.445 re-

spectively, selected to have similar numbers of sources. The stacking analysis has also been performed on the subsample of radio sources with available optical spectroscopy and diagnostic line ratios typical of star-formation activity. For this subsample we only consider star-forming sources with $z < 0.3$. At this redshift range the H α emission-line lies within the observable window of the spectroscopic observations allowing reliable classification on the basis of diagnostic emission-line ratios. The stacking analysis of this subsample will allow us to investigate whether Seyfert-2s that remain unidentified due to the absence of optical spectroscopy for many radio sources can significantly bias our conclusions.

The stacking results for the above subsamples in both the soft and the hard bands are presented in Table 1. The X-ray flux in this table is estimated from the raw net counts after correcting individual galaxies for (i) the effect of vignetting estimated from the corresponding exposure map and (ii) the energy fraction outside the adopted aperture of 10 arcsec using the encircled energy corrections recently derived by Ghizzardi (2001a, 2001b) for both the PN and the MOS detectors (see section 3). The counts-to-flux conversion factor has been derived assuming a power-law with spectral index $\Gamma = 2.0$ and Galactic absorption (see section 3). The X-ray luminosities in Table 1 are estimated using the X-ray flux derived from the stacking analysis and the median redshift of each subsample also listed in this table. The k-correction is estimated for a power-law with spectral index $\Gamma = 2.0$. Both the X-ray flux and luminosity are corrected for Galactic photoelectric absorption ($N_H = 2 \times 10^{20}$ cm $^{-2}$) but not for intrinsic absorption. The L_B and $L_{1.4}$ in Table 1 are the medians of the rest frame luminosities of individual galaxies. The B -band k-correction for a given radio source is derived from the best fit SED estimated by HYPER-Z. At 1.4 GHz we assume a power law SED of the form $f_\nu \sim \nu^{-0.8}$ to calculate the k-correction and to estimate the rest frame $L_{1.4}$ of individual radio sources.

In the soft-band a statistically significant signal is obtained for all the subsamples in Table 1. Stacking of the hard band counts, gives a marginally significant signal for the high redshift subsample at the 2.6σ confidence level. For the whole sample the hard band stacked signal is significant at the 1.9σ level but this is primarily due to high- z rather than low- z sources. The marginally significant hard band signal of the $z = 0.3 - 0.8$ sub-sample may be due to contamination by few AGNs that lie just below the detection threshold. This is further discussed below. Alternatively this may suggest hardening of the mean X-ray properties of radio sources at higher redshifts and/or at higher radio powers. It is thus possible that the present high- z radio subsample has X-ray spectral properties different to those of the low- z one. Deeper X-ray data are required to provide stronger constraints on the X-ray spectral properties of the $z = 0.3 - 0.8$ radio sources.

For the 2–8 keV band 3σ upper limits are estimated for the stacked signal assuming Poisson statistics. Also, spectroscopically confirmed star-forming radio sources exhibit a statistically significant stacked signal and have 0.5–2 keV X-ray flux and luminosity similar to that obtained for the $z = 0.0 - 0.3$ subsample spanning a similar redshift range. This suggests that powerful AGNs do not significantly bias our results at least for the $z = 0.0 - 0.3$ redshift bin.

Comparison of the estimated soft-band count rates with

redshift range	median redshift	source number	S+B ^a		B ^b		SNR ^c		< f_X > ^d		< L_X > ^e		L_B^f	$L_{1.4}^g$
			SB	HB	SB	HB	SB	HB	SB	HB	SB	HB		
0.0–0.8	0.291	34	467	380	365.3	345.1	5.3	1.9	2.9 ± 1.0	< 10.3	6.8 ± 2.3	< 24.5	1.39	5.0
0.0–0.3	0.240	19	267	204	208.1	199.7	4.1	0.3	3.0 ± 1.4	< 9.5	4.8 ± 2.2	< 15.2	1.38	2.0
0.3–0.8	0.445	15	200	176	157.2	145.3	3.4	2.6	2.7 ± 1.4	< 17.0	15.4 ± 7.8	< 98.6	1.40	6.3
0.0–0.3 ^h	0.177	6	86	52	58.89	55.7	3.5	-0.5	5.9 ± 2.9	< 16.9	5.0 ± 2.5	< 14.4	1.61	1.0

^aSource+Background counts in the soft (SB) and the hard (HB) bands

^bBackground counts in the soft (SB) and the hard (HB) bands

^cSignificance of detection in background standard deviations in the soft (SB) and the hard (HB) bands

^dX-ray flux in units of $10^{-16} \text{ erg s}^{-1} \text{ cm}^{-2}$ in the soft (SB) and the hard (HB) bands

^eX-ray luminosity in units of $10^{40} \text{ erg s}^{-1}$ in the soft (SB) and the hard (HB) bands

^fB-band luminosity in units of $10^{43} \text{ erg s}^{-1}$

^g1.4 GHz luminosity density in units of $10^{22} \text{ W Hz}^{-1}$

^hSpectroscopically confirmed star-forming galaxies on the basis of diagnostic line ratios

Table 1. Stacking analysis results in the soft (0.5–2 keV) and hard (2–8 keV) bands for the different samples of the Phoenix/XMM faint radio galaxies.

the hard-band upper limits can constrain the spectral properties of the sub-mJy radio sources with spiral galaxy SEDs. For the $z = 0.0 - 0.3$ redshift bin the observed count rates at the median redshift $z = 0.240$ translate to an upper limit of $N_H \approx 4 \times 10^{21} \text{ cm}^{-2}$ assuming a power law with spectral index $\Gamma = 1.7$. This increases to $N_H \approx 8 \times 10^{21} \text{ cm}^{-2}$ for $\Gamma = 2$. By constraining the column density to the Galactic value of $N_H = 2 \times 10^{20} \text{ cm}^{-2}$ a lower limit to the spectral index $\Gamma > 1.3$ is inferred. These constraints, although not very tight, are consistent with the spectral properties of nearby star-forming spirals (e.g. Fabbiano 1989). For the $z = 0.3 - 0.8$ subsample, the observed count rates translate to an upper limit of $N_H \approx 1 \times 10^{22} \text{ cm}^{-2}$ assuming a spectral index $\Gamma = 1.7$. This will increase to $N_H = 2 \times 10^{22} \text{ cm}^{-2}$ for $\Gamma = 2$. Keeping the column density constant at the Galactic value $N_H \approx 2 \times 10^{20} \text{ cm}^{-2}$ we find a lower limit to the spectral index $\Gamma > 0.8$. If the marginally significant hard band count rate is taken at face value, however, we estimate a hydrogen column density of $N_H \approx 1 \times 10^{22} \text{ cm}^{-2}$ ($\Gamma \approx 2.0$). This column density may indicate either low-luminosity AGN (LLAGN) activity or heavily obscured AGN/star-formation for the $z = 0.3 - 0.8$ subsample. Using the empirical relation between X-ray absorption and optical extinction of Gorenstein (1975) the above column density translates to $E(B-V) \approx 1.4$. Leech et al. (1988) obtained optical spectra for high Galactic latitude IRAS sources (both starbursts and AGNs) and found a mean $E(B-V) \approx 1.3$ comparable to the reddening estimated here. Veilleux et al. (1995) used high quality nuclear optical spectra of luminous IRAS sources. For the sub-sample classified H II galaxies they estimate a mean $E(B-V) \approx 1$ which is somewhat lower than the value estimated here.

We also investigate the possibility that the observed stacked signal is primarily due to a few bright X-ray sources below the detection threshold. This is important especially if some of these sources are AGNs and thus not representative of the star-forming galaxy population studied in this paper. We explore this issue by assigning detection significances to individual radio sources and then excluding sources above a given threshold. The detection significance is calculated by the ratio of net source counts to the square root of the background estimated as described in section 5.

For the whole ($z = 0.0 - 0.8$) sample a significant 0.5–2 keV signal is still obtained after removing sources above 3σ (total of 3). These sources have relatively low X-ray-to-optical luminosity ratios $\log L_X/L_B \approx -2$, typical of starbursts. Clearly, deeper X-ray observations are required to further address this issue.

For the 2–8 keV band all sources have hard band detection significances below the 3σ level. Removing the 3 higher significance sources ($> 1.7\sigma$) reduces the confidence level of the hard band stacked signal to $\approx 1\sigma$ for both the $z = 0.0 - 0.8$ and $z = 0.3 - 0.8$ subsamples respectively. Therefore, it is possible that contamination by few obscured AGNs is responsible for the apparent hardening of the mean X-ray spectral properties of the high- z sub-sample.

We note that for flat Λ cosmology ($\Omega_M = 0.3$, $\Omega_\Lambda = 0.7$) the luminosities estimated in Table 1 will increase by ≈ 24 and ≈ 40 per cent for the $z = 0.0 - 0.3$ and $z = 0.3 - 0.8$ subsamples respectively

7 AGN CONTAMINATION

The aim of the present paper is to explore the mean properties of star-forming sub-mJy radio galaxies and we have attempted to exclude sources that show evidence for strong AGN activity from the sample used in the stacking analysis. We argue that the AGN contamination of the present radio selected sample is small:

- Radio selection at μJy flux densities has been shown to be efficient in finding actively star-forming systems to $z \approx 1$. Only $\approx 10 - 20$ per cent of the faint radio population are believed to be AGNs (Georgakakis et al. 1999; Barger et al. 2002; Bauer et al. 2002; Chapman et al. 2003).

- A total of 7 radio sources with optical counterparts exhibiting unresolved light profiles in the R -band, likely to be distant QSOs, have been identified and excluded from the sample.

- Within the spectroscopic sample only 5 out of the 31 radio sources with spectroscopic observations show evidence for Seyfert-1 or 2 type activity. One of these sources is a distant ($z \approx 1.9$) QSO, another source is classified Seyfert-2 on the basis of diagnostic optical emission line ratios and the re-

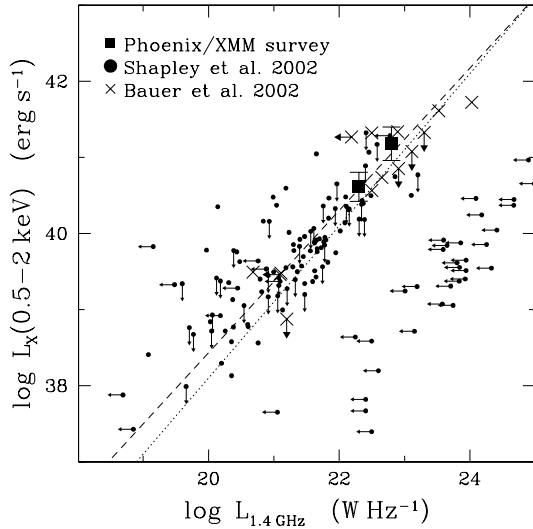


Figure 3. Soft band 0.5–2 keV X-ray luminosity against 1.4 GHz radio power. The stacking analysis results for the PDS radio sources in the redshift range $z = 0.05–0.3$ and $0.3–0.8$ are shown with the filled squares. The small filled circles are local galaxies from the sample compiled by Shapley et al. (2001). The crosses are star-forming faint radio sources from the sample of Bauer et al. (2002). The dashed line shows the best fit $L_X - L_{1.4}$ relation derived by Bauer et al. (2002) shifted to the 0.5–2 keV band as described in the text. The dotted line is the best fit $L_X - L_{1.4}$ relation derived by Ranalli et al. (2003).

maintaining three belong to the group of spectroscopically “unclassified” sources (see section 2). These three sources have X-ray counterparts with X-ray spectral properties indicative of AGN activity (e.g. hard X-ray spectra, X-ray luminosities in excess of $\approx 10^{42} \text{ erg s}^{-1}$). All of these sources have been excluded from the stacking analysis.

- For the group of spectroscopically “unclassified” radio sources (see section 2) *without* X-ray counterparts to the sensitivity limit of the existing observations (total of 9) we can constrain their nature by estimating upper limits to their L_X/L_B and L_X . For sources with $z < 0.4$ (4 out of 9) we find $\log f_X/f_{\text{opt}} < -2$ and $L_X(0.5 - 2 \text{ keV}) < 2 \times 10^{41} \text{ erg s}^{-1}$ consistent with star-formation rather than AGN activity. For sources with $z > 0.4$ (5 out of 9) the estimated upper limits are not as stringent: most of these sources typically have $\log f_X/f_{\text{opt}} < -1.2$ and $L_X(0.5 - 2 \text{ keV}) < 5 \times 10^{41} \text{ erg s}^{-1}$. These limits exclude the possibility of powerful AGNs and suggest starbursts, obscured AGNs or LLAGNs. In the case of obscured AGNs the soft 0.5–2 keV band X-ray emission from the AGN is expected to be heavily obscured. The X-ray emission in the 0.5–2 keV spectral band is thus likely to be dominated by stellar processes (e.g. NGC 6240; Vignati et al. 1999). Deeper X-ray observations are required to elucidate the detailed nature of these sources. Nevertheless, the $z < 0.4$ sub-sample for which our observations can put tight constraints is dominated by star-formation.

- In Table 1 we estimate mean X-ray-to-optical luminosity ratios of $\log L_X/L_B \approx -2.4$ and -2.0 for the 0.240 and 0.445 redshift subsamples respectively. These ratios although elevated compared to those found for optically selected spiral galaxy samples (Hornschemeier et al. 2002a;

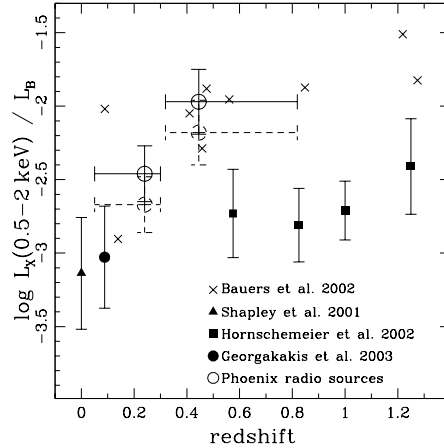


Figure 4. $\log L_X(0.5 - 2 \text{ keV})/L_B$ against redshift. Open circles are the stacking analysis results for the late type (Sbc, Scd and Im) PDS radio sources in the redshift range $z = 0.05 - 0.3$ and $0.3 - 0.8$. The points are plotted at the median z , while the horizontal errorbars indicate the extent of the redshift bins. The dashed line symbols represent our stacking analysis $\log L_X/L_B$ estimates after correcting for the difference in L_B between optical and radio selected samples (see text for details). Also shown are the mean $\log L_X/L_B$ of local spirals (triangles; Shapley et al. 2001), $z \approx 0.1$ spirals (filled circle; Georgakakis et al. 2003) and the stacking analysis results for distant late type galaxies in the *Chandra* Deep Field North (squares; Hornschemeier 2002a). The crosses are the $\log L_X/L_B$ ratio for narrow emission line radio galaxies in the *Chandra* Deep Field North from the sample of Bauer et al. (2002).

Georgakakis et al. 2003) are typical of actively star-forming galaxies rather than AGN dominated systems (Alexander et al. 2002). Moreover, the 0.5–2 keV X-ray luminosities in the two redshift bins are $\approx 5 \times 10^{40}$ and $\approx 1.5 \times 10^{41} \text{ erg s}^{-1}$ respectively. These luminosities are intermediate to Milky Way type spirals ($\approx 10^{40} \text{ erg s}^{-1}$; Warwick et al. 2002) and luminous starbursts like NGC 3256 ($\approx 10^{42} \text{ erg s}^{-1}$; Moran, Lehnert & Helfand 1999).

- The estimated mean X-ray flux ($f_X(0.5 - 2 \text{ keV}) = 5.9 \times 10^{-16} \text{ erg s}^{-1} \text{ cm}^{-2}$) and luminosity ($L_X(0.5 - 2 \text{ keV}) = 5.0 \times 10^{40} \text{ erg s}^{-1}$) of spectroscopically confirmed $z < 0.3$ star-forming radio sources (see Table 1) are similar to those obtained for the *all* $z < 0.3$ radio sources with spiral SEDs ($f_X(0.5 - 2 \text{ keV}) = 3.1 \times 10^{-16} \text{ erg s}^{-1} \text{ cm}^{-2}$; $L_X(0.5 - 2 \text{ keV}) = 4.8 \times 10^{40} \text{ erg s}^{-1}$). Hence, any contribution from AGNs/QSOs at least for the $z = 0.0 - 0.3$ subsample is minimal.

- The mean X-ray and radio luminosities of the faint radio sources studied here are consistent with the $L_X - L_{1.4}$ correlation of local star-forming galaxies. This is discussed in detail in the next section.

The evidence above suggest that the detected stacked X-ray signal is consistent with star-formation activity. However, despite our effort to minimise the AGN contamination we cannot exclude the possibility of a small fraction of low-luminosity or obscured AGNs within our radio selected sample.

8 DISCUSSION

8.1 X-ray properties of the faint radio population

The sub-mJy and μ Jy radio population is believed to comprise a large fraction of starburst galaxies out to $z \approx 1$ (Benn et al. 1993; Hopkins et al. 1998; Georgakakis et al. 1999; Chapman et al. 2003). The enhanced SFR in these systems results in increased radio emission due to both thermal emission and synchrotron radiation in supernovae remnants. Moreover, studies of local star-forming and spiral galaxies demonstrate that these systems are also powerful X-ray emitters (Fabbiano 1989; Read, Ponman & Strickland 1997; Dahlem, Weaver & Heckman 1998; Read & Ponman 2001) with luminosities that in some cases exceed $\approx 10^{42} \text{ erg s}^{-1}$ (e.g. NGC 3265; Moran et al. 1999). The X-ray emission in these galaxies originates from a combination of evolved stellar point sources (X-ray binaries) and diffuse hot ($T \approx 1 - 8 \times 10^6 \text{ K}$) gas heated by supernovae shocks (Read, Ponman & Strickland 1997; Read & Ponman 2001). Since the physical processes giving rise to both the X-ray and the radio emission have the same origin, i.e. enhanced SFR, a correlation should be expected between the X-ray and radio luminosities of star-forming galaxies and sub-mJy radio sources.

Shapley, Fabbiano & Eskridge (2001) compiled a large sample of local spirals with X-ray data from the *Einstein* observatory and multiwavelength observations. They find a highly significant correlation between the X-ray and radio luminosities suggesting an association between X-ray emission and star-formation activity. However, although Shapley et al. (2001) exclude AGN dominated systems from the analysis, their sample may be contaminated by LLAGNs. Ranalli et al. (2003) used the atlas of optical nuclear spectra of Ho et al. (1997) to compile a carefully selected sample of nearby star-forming galaxies with available X-ray and radio data. The advantage of their sample is that the high quality nuclear spectra of Ho et al. (1997) provide reliable spectral classification of the central source (star-formation/AGN) thus, minimising the contamination from LLAGN. Moreover, use of *ASCA* and *BeppoSAX* X-ray data allow Ranalli et al. (2003) to extend their study of star-forming galaxies to hard X-rays (2–10 keV). These authors report a tight correlation between radio power (1.4 GHz) and X-ray luminosity in both the 0.5–2 and the 2–10 keV spectral bands.

Bauer et al. (2002) investigated the association between faint X-ray and radio source populations detected in the 1 Ms *Chandra* Deep Field North (CDF-N). They found that the majority of X-ray sources with narrow emission-line spectra also have μ Jy radio counterparts and are likely to be dominated by star-formation activity. Also, for the star-forming galaxy subsample they find a $L_X - L_{1.4}$ relation similar to that obtained by Shapley et al. (2001) for local non-AGN spirals. They argue that the evidence above suggests that the local $L_X - L_{1.4}$ can be extended to intermediate and high redshifts and that the X-ray emission of narrow emission line X-ray sources is associated with star-formation activity.

Figure 3 plots 1.4 GHz radio power against 0.5–2 keV X-ray luminosity for both the Shapley et al. (2001) local spirals and the Bauer et al. (2002) distant sub-mJy radio sources with narrow emission line spectra. To transform the X-ray luminosities of the above samples to the 0.5–2 keV band used

in the present study we assume a power-law model with a spectral index $\Gamma = 2.0$. At radio wavelengths a power-law spectral energy distribution of the form $f_\nu \sim \nu^{-0.8}$ appropriate for star-forming galaxies is adopted to convert the 4.85 GHz radio flux density of Shapley et al. (2001) to 1.4 GHz. Also shown in Figure 3 are the stacking analysis results of the PDS sub-mJy radio sources in the $z = 0.0 - 0.3$ and $z = 0.3 - 0.8$ redshift bins. It is clear that there is excellent agreement between the mean X-ray and 1.4 GHz luminosities derived here and the $L_X - L_{1.4}$ relation of Bauer et al. (2002) and Ranalli et al. (2003) for star-forming galaxies. This suggests that the present sample of sub-mJy radio sources to $z \approx 0.5$ is dominated by starburst rather than AGN activity. Indeed, AGN dominated systems as well as LLAGNs have X-ray-to-radio luminosity ratios elevated compared to those of star-forming galaxies (Brinkmann et al. 2000; Alexander et al. 2002; Ranalli et al. 2003).

To further investigate the nature of the faint radio sources we use their X-ray-to-optical luminosity ratios. Figure 4 plots the mean L_X/L_B ratio of the present sample against redshift in comparison with optically selected ‘normal’ spirals. It is clear that faint radio sources have elevated L_X/L_B ratios by a factor of 2–10 compared to optically selected spiral galaxy samples. This is partly due to the enhanced mean L_B of the present sample in combination with the non-linear correlation between optical and X-ray luminosities $L_X \approx L_B^{1.5}$ reported by Shapley et al. (2001). Accounting for the differences in the mean L_B of radio and optically selected samples will decrease our L_X/L_B estimates by about 0.2 in log space. The corrected L_X/L_B ratios are still somewhat elevated compared to those of Georgakakis et al. (2003) and Hornschemeier et al. (2002a) samples. This may suggest elevated star-formation activity in the radio selected sample. Nevertheless, the apparent difference is not statistically significant. Indeed, within the errors the L_X/L_B ratio is roughly constant with redshift suggesting that the L_X of star-forming galaxies evolves with redshift in the same rate as L_B .

Moreover, the difference in the L_X/L_B between low and high- z radio selected sub-samples, although not very significant, may suggest enhanced galaxy activity with increasing redshift or radio power. Also shown in this Figure 4 are the L_X/L_B ratios of individual CDF-N narrow-emission line radio sources with X-ray counterparts (Bauer et al. 2002). We use the *I*-band magnitudes given by Bauer et al. (2002) to estimate rest-frame *B*-band luminosity using the SED of Sbc type galaxies. There is good agreement between the L_X/L_B of the CDF-N X-ray detected radio sources and our stacking analysis results.

Finally, the analysis above suggests that sub-mJy spiral galaxies have X-ray properties similar to those of X-ray detected narrow emission-line galaxies. Indeed, many of these sources also appear to reside in disc galaxies with blue optical colours and enhanced X-ray emission relative to the optical (McHardy et al. 1998), while their optical spectra and X-ray properties suggest a mix of star-forming galaxies and obscured AGNs. Therefore, sub-mJy galaxies and at least a fraction of the X-ray selected narrow emission-line galaxies are drawn from the same parent population. This is in agreement with Bauer et al. (2002) who find a large overlap between the faint X-ray and radio selected populations especially for the sources with narrow emission line spectra.

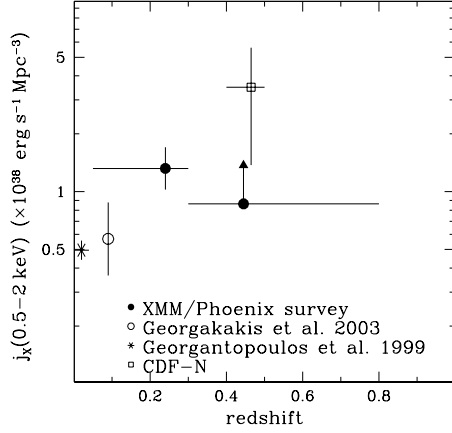


Figure 5. 0.5–2 keV X-ray emissivity, j_X , against redshift. Filled circles are the sub-mJy star-forming radio sources from the Phoenix/XMM survey in the redshift bins $z = 0.05 - 0.3$ and $0.3 - 0.8$. These points are plotted at the median z , while the horizontal errorbars indicate the extent of each bin. The open circle represents optically selected spirals at $z \approx 0.1$ from the 2dF Galaxy Redshift Survey (Georgakakis et al. 2003). The star corresponds to local star-forming systems (Georgantopoulos et al. 1999). The open square is the j_X estimate for narrow emission line radio sources with X-ray counterparts detected in the CDF-N (see text for details). Although the uncertainties are large, there is evidence for evolution of j_X to $z \approx 0.3$ of the form $(1+z)^3$. At higher redshifts the Phoenix/XMM survey is affected by incompleteness allowing only a lower limit for j_X to be estimated. The CDF-N point at $z \approx 0.5$ provides some evidence for evolution at $z > 0.3$ but the large uncertainty (due to small number statistics) do not allow firm conclusions to be drawn.

They argue that these galaxies are most likely normal and starburst spirals in the redshift range $z \approx 0.3 - 1.3$.

8.2 X-ray emissivity of sub-mJy galaxies

The emissivity of galaxy samples selected at various wavelengths (UV, optical, radio) over a range of redshifts is one of the most powerful and widely used evolutionary tests (e.g. Lilly et al. 1996; Connolly et al. 1997).

The X-ray emissivity, j_X , of star-forming systems has been estimated locally by Georgantopoulos, Basilakos & Plionis (1999). They convolved the local optical luminosity function of the Ho et al. (1995) sample with the corresponding $L_X - L_B$ relation based on *Einstein* data. The Ho et al. sample has the advantage of high S/N nuclear optical spectra and hence, reliable spectral classifications (Ho et al. 1997) necessary to study the properties of star-forming systems. Recently, Georgakakis et al. (2003) compiled a sample of ‘normal’ spirals from the 2dF Galaxy Redshift Survey and used stacking analysis to estimate their j_X at $z \approx 0.1$. The Phoenix/XMM survey provides the opportunity to extend these results to higher redshifts, assuming that the present sample of sub-mJy sources is indeed dominated by star-formation activity.

For the j_X determination, we first need to estimate the effective cosmological volume probed by the present radio selected sample corrected for optical and radio selection biases (e.g. $R < 21.5$ mag, $S_{1.4} > 80 \mu\text{Jy}$) using the stan-

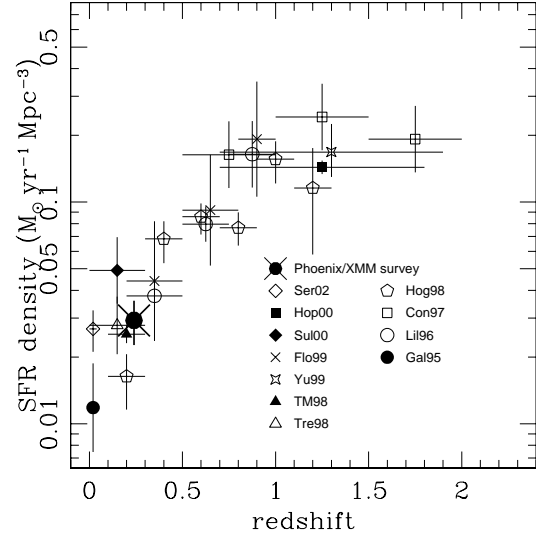


Figure 6. Global star-formation density against redshift estimated from galaxy samples selected at various wavelengths. SFR dependent reddening corrections have been applied to the data as described in Hopkins et al. (2001). References in this diagram are as follows: Ser02: Serjeant et al. 2002; Hop00: Hopkins et al. 2000; Sul00: Sullivan et al. 2000; Flo99: Flores et al. 1999; Yan99: Yan et al. 1999; TM98: Tresse & Maddox (1998); Tre98: Treyer et al. 1998; Hog98: Hogg et al. 1998; Con97: Connolly et al. (1997); Lil96: Lilly et al. 1996; Gal95: Gallego et al. (1995). The SFR density estimated in the present study using stacking analysis is shown with the crossed filled circle. No absorption corrections have been applied. Given the uncertainty in converting X-ray luminosities to star-formation rates the agreement of our estimate at $z \approx 0.3$ with previous studies is encouraging.

dard $1/V_{max}$ formalism (e.g. Lilly et al. 1996; Mobasher et al. 1999). We also account for radio catalogue incompleteness due to (i) the varying sensitivity of the radio observations across the field (weighting correction) and (ii) extended low surface brightness radio sources with total flux density above the survey limit that can be missed by the detection algorithm (resolution correction). These biases as well as methods to correct for them are fully described by Hopkins et al. (1998). We note that the rms noise level of the radio observations is relatively uniform over the area of the Phoenix/XMM field and the resulting weighting correction is small. Finally in estimating j_X we also assume that the sub-mJy radio sources have constant $L_X/L_{1.4}$ ratio as indicated in Figure 3.

We estimate soft-band 0.5–2 keV emissivities of $(1.3 \pm 0.3) \times 10^{38}$ and $(0.9 \pm 0.1) \times 10^{38} \text{ erg s}^{-1} \text{ Mpc}^{-3}$ for the late-type sub-mJy radio sources in the redshift bins $z = 0.0 - 0.3$ and $z = 0.3 - 0.8$ respectively. We note that the j_X estimate of the $z = 0.3 - 0.8$ subsample is a lower limit. This is mainly due to the fraction of sub-mJy radio sources in the $z = 0.3 - 0.8$ redshift range and optical magnitudes fainter than $R = 21.5$. Future optical observations reaching fainter magnitude limits will help address this issue. Moreover, radio sources at a given redshift with radio luminosity fainter than the survey limit are missed in the j_X calculation. We estimate the magnitude of this effect using the evolving radio luminosity function of Rowan-Robinson et al.

(1993) that has been shown to reproduce the observed radio source counts below 1 mJy (Hopkins et al. 1998). We find this bias to be small for the $z = 0.0 - 0.3$ redshift bin: correcting for the radio sources fainter than the survey limit increases j_X by less than about 10 per cent. However, for the $z = 0.3 - 0.8$ bin this effect is larger, ≈ 30 per cent. For flat Λ cosmology ($\Omega_M = 0.3$, $\Omega_\Lambda = 0.7$) the j_X estimated here will decrease by ≈ 10 and ≈ 30 per cent for the $z = 0.0 - 0.3$ and $z = 0.3 - 0.8$ subsamples respectively.

Figure 5 plots the X-ray emissivity of the sub-mJy radio sources against redshift in comparison with that of local star-forming galaxies (Georgantopoulos et al. 1999; scaled to the 0.5–2 keV band) and $z \approx 0.1$ 2dF Galaxy Redshift Survey spirals (Georgakakis et al. 2003). It is clear that the j_X in Figure 5 increases from the local Universe to $z \approx 0.3$, suggesting evolution. At higher redshifts, as already mentioned, the present study cannot further constrain the j_X evolution, although with deeper optical observations of the Phoenix/XMM field this issue may be addressed. At redshifts $z > 0.3$ we provide additional constraints on the X-ray evolution of star-forming galaxies using the sub-sample of narrow emission line radio sources with X-ray counterparts in the CDF-N presented by Bauer et al. (2002). These authors argue that the properties of these radio galaxies are consistent with star-formation activity dominating their X-ray emission. In the j_X calculation we consider sources in the redshift range $0.4 < z < 0.5$ with $S_{1.4} > 50 \mu\text{Jy}$ (i.e. the 5σ radio completeness limit) and $f_X(0.5 - 8 \text{ keV}) > 1 \times 10^{-16} \text{ erg s}^{-1} \text{ cm}^{-2}$ (X-ray detection limit). Only 4 sources in the Bauer et al. (2002) sample satisfy these criteria and therefore the estimated j_X plotted in Figure 5 suffers from large uncertainties. Despite the small number statistics the j_X of the CDF-N X-ray detected radio sources at $z \approx 0.5$ is elevated compared to both local spirals and $z \approx 0.3$ radio sources. The significance level of this result is low but it is interesting that to the first approximation the j_X of X-ray detected radio sources is in broad agreement with the stacking analysis results presented here.

Under the assumption that the faint radio population is indeed dominated by star-formation activity, the observed increase in j_X at least to $z \approx 0.3$ suggests an evolutionary rate of the form $(1+z)^3$ broadly consistent with the Peak-M models of Ghosh & White (2001). This set of models is also in agreement with the stacking analysis results of $z \approx 0.5$ spirals of Brandt et al. (2001b).

Assuming that the faint radio population is dominated by star-formation activity (as the present study indicates) the increase in j_X with redshift is attributed to the evolution of the global star-formation rate. Using the empirical relation $\text{SFR} = 2.2 \times 10^{-40} \times L_X(0.5 - 2 \text{ keV}) \text{ M}_\odot \text{ yr}^{-1}$ (Ranalli et al. 2003) we estimate a SFR density of $0.029 \pm 0.007 \text{ M}_\odot \text{ yr}^{-1} \text{ Mpc}^{-3}$ for the $z = 0.0 - 0.3$ redshift bin at a median redshift of 0.240 in good agreement with previous studies selecting star-forming galaxies at UV, optical or radio wavelengths. This is demonstrated in Figure 6, showing the SFR density as a function of redshift.

9 CONCLUSIONS

In this paper we apply stacking analysis to study the mean X-ray properties of sub-mJy radio galaxies using a 50 ks

XMM-Newton pointing overlapping with a subregion of a deep and homogeneous radio survey reaching μJy sensitivities (Phoenix Deep Survey). Multiwavelength UV, optical and NIR photometric data are available for this field allowing photometric redshifts and spectral types (i.e. ellipticals, spirals) to be estimated for all radio sources brighter than $R = 21.5$ mag (total of 82).

The subsample of $R < 21.5$ mag faint radio sources with spiral galaxy SEDs (total of 34, after excluding AGN dominated sources) is segregated into two redshift bins with a median of $z = 0.240$ and 0.455 respectively. Stacking analysis is used to study the mean X-ray properties of the sources in each redshift subsample. In the 0.5–2 keV soft band a statistically significant signal is obtained for both the low and the high- z subsamples. Stacking of the hard band counts yields a marginally significant signal (2.6σ) for the $z = 0.455$ subsample only.

We argue that the AGN contamination of our sample is minimal on the basis of the following arguments:

- (i) Radio selection at μJy flux densities has been shown to be efficient in finding actively star-forming systems to $z \approx 1$. Only $\approx 10 - 20$ per cent of the faint radio population are believed to be AGNs.
- (ii) Radio sources with optical counterparts exhibiting unresolved optical light profile, likely to be distant QSOs, have been identified and excluded from the sample.
- (iii) Radio sources having X-ray counterparts with X-ray properties suggesting AGN activity have been excluded from the stacking analysis. Similarly, faint radio sources with optical spectral features (e.g. diagnostic emission line ratios, broad optical lines) typical of AGNs have also been excluded from the stacking sample.
- (iv) The mean X-ray properties of spectroscopically confirmed star-forming radio sources at $z < 0.3$ are similar to those obtained for the *whole* sample of $z < 0.3$ radio sources with spiral galaxy SEDs.
- (v) The mean X-ray and radio luminosities of the faint radio sources studied here are consistent with the $L_X - L_{1.4}$ correlation of local star-forming galaxies.
- (vi) The mean X-ray luminosity and X-ray-to-optical flux ratio of the present faint radio sample are consistent with star-formation rather than AGN activity.

Although the evidence above suggests that the observed X-ray emission is dominated by star-formation activity we cannot exclude the possibility of contamination of the present sample by a small number of low-luminosity or heavily obscured AGN. Our main conclusions are summarised below:

- The mean L_X/L_B ratio of the faint radio population studied here is elevated compared to optically selected spirals in the redshift range $0 < z < 1$. Differences in the L_B distributions of the samples can partly compensate for this effect. Elevated star-formation activity in the radio selected sample may also be responsible for the increased L_X/L_B .
- There is some evidence of increasing L_X/L_B with increasing redshift or $L_{1.4}$ for the sub-mJy galaxies. Although the uncertainties hamper a secure interpretation this may suggest that more energetic systems (in terms of X-ray-to-optical flux ratio) are also more powerful radio emitters.
- We find strong evidence for enhanced X-ray emissivity

of sub-mJy sources to $z \approx 0.3$ compared to local HII galaxies and $z \approx 0.1$ spirals. This increase is consistent with X-ray evolution of the form $\approx (1+z)^3$. If the present sample of faint radio sources to $z \approx 0.3$ is indeed dominated by star-formation then this is the first direct evidence for evolution of these systems at X-ray wavelengths. At $z > 0.3$ incompleteness affects our results and the present data cannot be used to constrain the evolution in this regime.

• Using an empirical X-ray luminosity to SFR conversion factor we estimate a global SFR density of $0.029 \pm 0.007 M_{\odot} \text{ yr}^{-1} \text{ Mpc}^{-3}$ at $z \approx 0.3$. This is found to be in fair agreement with previous studies.

10 ACKNOWLEDGMENTS

We thank the anonymous referee for constructive comments. This work is jointly funded by the European Union and the Greek Government in the framework of the programme “Promotion of Excellence in Technological Development and Research”, project “X-ray Astrophysics with ESA’s mission XMM”. AMH acknowledges support provided by the National Aeronautics and Space Administration through Hubble Fellowship grant HST-HF-01140.01-A awarded by the Space Telescope Science Institute. JA gratefully acknowledges the support from the Science and Technology Foundation (FCT, Portugal) through the fellowship BPD-5535-2001 and the research grant POCTI-FNU-43805-2001.

REFERENCES

- Alexander D. M., Aussel H., Bauer F. E., Brandt W. N., Hornschemeier A. E., Vignali C., Garmire G. P., Schneider D. P., 2002, *ApJ*, 568L, 85
- Bauer F. E., Alexander D. M., Brandt W. N., Hornschemeier A. E., Vignali C., Garmire G. P., Schneider D. P., 2002, *AJ*, 124, 2351
- Bell E. F., 2003, *ApJ*, 586, 794
- Benn C. R., Rowan-Robinson M., McMahon R. G., Broadhurst T. J., Lawrence A., 1993, *MNRAS*, 263, 98
- Bolzonella M., Miralles J.-M., Pelló R., 2000, *A&A* 363, 476
- Brandt W. N. et al., 2001a, *AJ*, 122, 2810
- Brandt W. N., Hornschemeier A. E., Alexander D. M., Garmire G. P., Schneider D. P., Broos P. S., Townsley L. K., Bautz M. W., Feigelson E. D., Griffiths R. E., 2001b, *AJ*, 122, 1
- Brinkmann W., Laurent-Muehleisen S. A., Voges W., Siebert J., Becker R. H., Brotherton M. S., White R. L., Gregg M. D., 2000, *A&A*, 356, 445
- Bruzual A. G., Charlot S., 1993, *ApJ*, 405, 538
- Chapman S. C., et al., 2003, *ApJ*, 585, 57.
- Coleman G. D., Wu C.-C., Weedman D. W., 1980, *ApJ*, 43, 393
- Condon, J. J., 1992, *ARA&A*, 30, 575
- Connolly A. J., Szalay A. S., Dickinson M., Subbarao M. U., Brunner R. J., 1997, *ApJ*, 486, 11L
- Dahlem M., Weaver K. A., Heckman T. M., 1998, *ApJS*, 118, 401
- David L. P., Jones C., Forman W., 1992, *ApJ*, 388, 82
- Gallego J., Zamorano J., Aragon-Salamanca A., Rego M., 1995, *ApJ*, 455, L1
- Georgakakis A., Georgantopoulos I., Stewart G. C., Shanks T., Boyle B. J., 2003, *MNRAS*, submitted
- Georgakakis A., Mobasher B., Cram L., Hopkins A., Lidman C., Rowan-Robinson M., 1999, *MNRAS*, 306, 708.
- Georgantopoulos I., Basilakos S., Plionis M., 1999, *MNRAS*, 305, L31
- Ghizzardi S., 2001a, EPIC-MCT-TN-0.11
- Ghizzardi S., 2001b, EPIC-MCT-TN-0.12
- Ghosh P., White N. E., 2001, *ApJ*, 559, 97
- Gorenstein P., 1975, *ApJ*, 198, 95
- Fabbiano, G., 1989, *ARA&A*, 27, 87
- Flores H., et al. 1999, *ApJ*, 517, 148
- Hasinger, G.; Altieri, B.; Arnaud, M. et al., 2001, *A&A*, 365L, 45
- Helou G., Soifer B. T., Rowan-Robinson M., 1985, *ApJ*, 298L, 7
- Ho L. C., Filippenko A. V., Sargent W., 1995, *ApJS*, 98, 477
- Ho L. C., Filippenko A. V., Sargent W., 1997, *ApJS*, 112, 315
- Hogg D. W., Cohen J. G., Blandford R., Pahre M. A., 1998, *ApJ*, 504, 622
- Hopkins A. M., Afonso J., Chan B., Cram L. E., Georgakakis A., Mobasher B., 2003, *AJ*, 125, 465
- Hopkins A. M., Connolly A. J., Haarsma D. B., Cram L. E., 2001, *AJ*, 122, 288
- Hopkins A. M., Connolly A. J., Szalay A. S., 2000, *AJ*, 120, 2843
- Hopkins A., Afonso J., Cram L., Mobasher B., 1999, *ApJ*, 519L, 59
- Hopkins A. M., Mobasher B., Cram L., Rowan-Robinson M., 1998, *MNRAS*, 296, 839H
- Hornschemeier A. E., Brandt W. N., Alexander D. M., Bauer F. E., Garmire G. P., Schneider D. P., Bautz M. W., Chartas G., 2002a, *ApJ*, 568, 82
- Hornschemeier A. E., Bauer F. E., Alexander D. M., Brandt W. N., Sargent W. L. W., Vignali C., Garmire G. P., Schneider D. P., 2002b, *astro-ph/0211487*
- Leech K. J., Lawrence A., Rowan-Robinson M., Walker D., Penston M. V., 1988, *MNRAS*, 231, 977
- Lilly S. J., Le Fevre O., Hammer F., Crampton D., 1996, *ApJ*, 460, L1
- Lumb D. H., Warwick R. S., Page M., De Luca A., 2002, *A&A*, 389, 93
- McHardy I. M., Jones L. R., Merrifield M. R., Mason K. O., Newsam A. M., Abraham R. G., Dalton G. B., Carrera F., Smith P. J., Rowan-Robinson M., Abraham, R. G., 1998, *MNRAS*, 295, 641
- Mobasher B., Cram L., Georgakakis A., Hopkins A., 1999, *MNRAS*, 308, 45
- Moran E. C., Lehnert M. D., Helfand D. J., 1999, *ApJ*, 526, 649
- Mushotzky R. F., Cowie L. L., Barger A. J., Arnaud K. A., 2000, *Nature* 404, 459
- Nandra K., Mushotzky R. F., Arnaud K., Steidel C. C., Adelberger K. L., Gardner J. P., Teplitz H. I., Windhorst R. A., 2002, *ApJ*, 576, 625
- Ranalli P., Comastri A., Setti G., 2003, *A&A*, 399, 39
- Read A. M., Ponman T. J., 2001, *MNRAS*, 328, 127
- Read A. M., Ponman T. J., Strickland D. K., 1997, *MNRAS*, 286, 626
- Rowan-Robinson M., Benn C. R., Lawrence A., McMahon R. G., & Broadhurst T. J., 1993, *MNRAS*, 263, 123
- Serjeant S., Gruppioni C., Oliver S., 2002, *MNRAS*, 330, 621
- Shapley A., Fabbiano G., Eskridge P. B., 2001, *ApJS*, 137, 139
- Strüder L., Briel U., Dennerl K., et al. 2001, *A&A*, 365, L18
- Sullivan M., Treyer M. A., Ellis R. S., Bridges T. J., Milliard B., Donas J., 2000, *MNRAS*, 312, 442
- Tresse L., Maddox S. J., 1998, *ApJ*, 495, 691
- Treyer M. A., Ellis R. S., Milliard B., Donas J., Bridges T. J., 1998, *MNRAS*, 300, 303
- Turner M. J. L., Abbey A., Arnaud M., et al., 2001, *A&A*, 365, L27
- Veilleux S., Kim D. C., Sanders D. B., Mazzarella J., M., Soifer B. T., 1995, *ApJS*, 98, 171
- Vignati P. et al., 1999, *A&A*, 349, L57
- Warwick R. S., 2002, *astro-ph/0203333*
- Wilson G., Cowie L. L., Barger A. J., Burke D. J., 2002, *AJ*, 124, 1258

Yan L., McCarthy P. J., Freudling W., Teplitz H. I., Malumuth
E. M., Weymann R. J., Malkan M. A., 1999, ApJ, 519L, 47